A Practical Equalizer for Cooperative Delay Diversity with Multiple Carrier Frequency Offsets

Feng Wang, Mary Ann Ingram
School of Electrical and Computer Engineering, Georgia Tech, Atlanta, Georgia 30332-0250
fwang73@gatech.edu, mai@ece.gatech.edu

***Abstract*—Cooperative transmission in wireless networks provides diversity gain in multipath fading environments. Among all the proposed cooperative transmission schemes, delay diversity has the advantage of needing less coordination and higher spectrum efficiency. However, in a distributed network, the asynchrony comes from both carrier frequency and symbol timing between the cooperating relays. In this paper, a minimum mean square error fractionally spaced decision feedback equalizer (MMSE-FS-DFE) is developed to extract the diversity with large multiple carrier frequency offsets, its performance approaches the case without multiple carrier frequency offsets. The front end design for the receiver in this scenario is discussed, and a practical frame structure is designed for carrier frequency offsets and channel estimation. A subblock-wise decision-directed adaptive least squares (LS) estimation method is developed to solve the problem caused by error in frequency offset estimation. The purpose of this paper is to provide a practical design for cooperative transmission (CT) with the delay diversity scheme.**

Keywords-Cooperative transmission, multiple carrier frequency offsets, fractionally spaced decision feedback equalizer

I. INTRODUCTION

Cooperative transmission (CT) [1], [2] has been studied as a way for one single-antenna radio to help another single-antenna radio to transmit a single message more reliably, to combat multipath fading in wireless communications. CT methods that involve concurrent transmission, which implies physical layer combining, have been demonstrated to be effective for range extension [3]. When different radios are transmitting concurrently, the received signal has multiple frequency and time offsets, relative to the receiver. This paper presents a receiver design that is robust to multiple carrier frequency offsets (CFOs).

To create diversity, the signal copies combined in the receiver must undergo uncorrelated fading. One way to create diversity is for the cooperators to transmit over orthogonal relay channels [2], with either coherent or noncoherent demodulation [4] or differential demodulation [5]. However the spectral efficiency of orthogonal transmission is low. Another way is distributed space time coding (DSTC) [6]-[9] or space frequency block coding (SFBC) [10], which improves the spectral efficiency. Transmit diversity with artificial delay [11] can be viewed as a special case of DSTC. A third is coded cooperation and turbo-coded cooperation [12], [13]. Generally, all these approaches use block-transmission and assume the channel is quasi-static and without multiple CFOs.

CT is essentially asynchronous in a distributive network. The asynchrony in carrier frequency between the cooperating relays comes from the natural differences in oscillators in general and from the Doppler frequency shifts in a mobile channel. Some works addressed this multiple CFOs problem. Cooperative Orthogonal Frequency Division Multiplexing (OFDM) transmission with CFO mitigation was proposed in [14], where a special OFDM symbol with a long CP was designed to mitigate the CFOs, however, the long CP leads to low spectral efficiency. A multiple CFO compensation symbol-rate decision feedback equalization (DFE) approach was supposed in [15] for delay diversity method [11]. In [16], a maximum likelihood sequence estimation (MLSE) equalizer based on the Viterbi algorithm was developed for multiple CFO compensation. These papers mentioned above that address multiple CFOs represent each CFO as a multiplicative complex exponential factor in symbol-spaced samples, assuming that a transmitter pulse shaping filter such as root raised cosine (RRC) filter, and a matched filter on the receiver side, such that the equivalent channel impulse response satisfies the Nyquist criterion, i.e. that the symbol-rate samples are intersymbol interference (ISI) free. Then the equivalent sampled matched filter (SMF) channel model was deduced. The simulation in [16] shows that such design is limited to small CFOs, such as a normalized CFO less than 0.06, and the performance will degrade severely when the CFO is larger. For a real world narrowband application such as wireless telemetry, the CFO may be significantly larger, for example, the frequency tolerance of ARIB STD-T67 is $\pm$ 4ppm [17], with an occupied bandwidth of 8.5kHz and operating frequency at 429MHz, the normalized CFO is about 0.4.

In this paper, based on the artificial delay diversity approach [11], we suggest a fractional spaced equalizer (FSE) which can compensate very large multiple CFOs in a narrow-band flat-fading and quasi-static channel. We assume a crystal with stability $\pm$ 10ppm is used in the 2.4GHz frequency band with a Baud rate of 64KBps; thus, the CFO could reach $\pm$ 24KHz and the normalized carrier frequency offset will be as large as $\pm$ 0.375. The front-end design was modified to accommodate such a large CFO, necessitating a wider band filter in the front end to capture the signal spectrum with multiple CFOs. The wider band filter creates the need for FSE. This use of the wider band front end with the FSE is the one of the main contributions of this paper. The other is the design of a vector phase estimator, which is like a multi-output phase locked loop that tracks the multiple phase errors caused by estimation errors for frequency offsets.

The authors gratefully acknowledge partial support for this research from the National Science Foundation, grant number CNS-1017984.

978-1-4577-2053-6/12/$31.00 ©2012 IEEE

II. SYSTEM MODEL

A. Cooperative Transmission

We consider the range extension CT scenario shown in Fig. 1, which consists of a source, a cluster of M relays, and a destination. The packet transmitted from the source to the relays, and then all the relays will transmit the same packet to the destination. The destination is assumed to be out of range of the source. An additional artificial delay is introduced by each relay, so as to simulate a frequency selective fading channel, the destination will receive multiple copies of the packet fired at different times and delay diversity can be extracted.

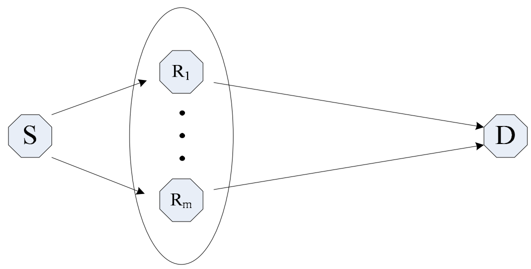

Fig. 1. Relay based cooperative transmission in network

We assume that the artificial delays are just multiples of the symbol period, and that the relays are symbol synchronized.

B. System Model for Relay-based Delay Diversity

Our system model is shown in Fig. 2, where each relay R_m has a carrier frequency offset Δf_m relative to the destination. β_m is the complex channel gain from relay R_m to the destination, with $m = 1, \cdots, M$. Narrow-band communication is assumed in this paper, so the channel gains from different transmitters to the receiver have flat fading, are assumed to be quasi-static, and are independent from each other. T is the symbol period, and τ_m is an integer to set the delay for relay R_m. a_k is the transmitted symbol at time index k, $w(t)$ is the additive white Gaussian noise (AWGN) in the channel.

An example passband frequency spectrum of the received signal $r(t)$ at the destination assuming $M = 2$ is illustrated in Fig. 3. The figure shows how the receiver matched filter and the SMF model response are mismatched for large CFOs, and now part of the valid signal would be filtered out. Instead, in this paper, we propose that the receiving filter $F(\omega)$ is an ideal flat wideband filter with baseband bandwidth $[-1/T, +1/T]$, which can accommodate the frequency-shifted signals.

The channel impulse response between the relay R_m and the destination node D without CFO is given by

$$h_k^{(m)} = \beta_m g_T(t_0^{(m)} + kT / F_0), \quad (1)$$

where $t_0^{(m)}$ is the timing phase, $g_T(t)$ is the transmitting pulse shaping filter, and F_0 is the over-sampling factor. If relay R_m and the destination node D are perfectly time synchronized, then $t_0^{(m)} = -\tau_m T$.

In our design, the transmitting pulse shaping filter $G_T(\omega)$ is a raised cosine (RC) filter with roll-off factor 0.22. Following the receiving filter is a sampler with sample rate of $2/T$. Note that a wider bandwidth for the receiving filter $F(\omega)$ and higher over-sampling factor can be chosen for even larger CFOs.

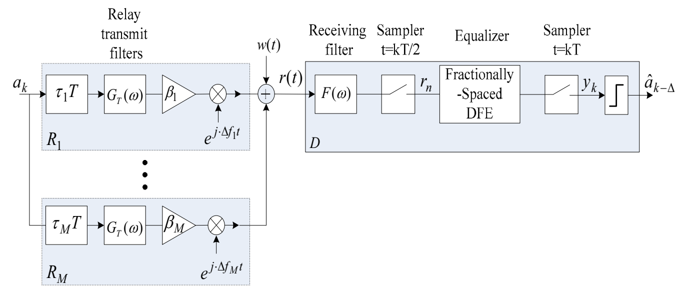

Fig. 2. System model for delay diversity

We note that the receiving filter $F(\omega)$ is an ideal rectangular window filter with edges at $f_c \pm 1/T$ in Fig. 2. The output noise at the receiver filter $F(\omega)$ is band-limited WGN, and the samples of the noise, w_k are independent zero-mean complex Gaussian random variables, with variance $\sigma_w^2 / 2$ in each of the real and imaginary parts. In a real application, the receiving filter $F(\omega)$ could be realized as a root raised cosine filter where the flat part of the filter should accommodate the received signal so no distortion will happen, and at the same time, the samples of the noise after this filter are independent random variables.

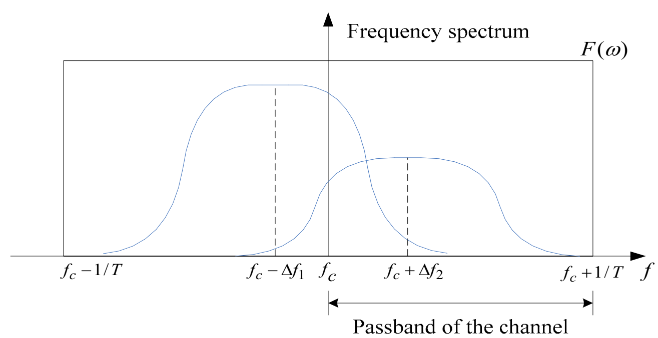

Fig. 3. Frequency spectrum of the received signal

The samples are fed into a FS-DFE, which is described in the next section.

III. EQUALIZER DESIGN

In [15], a symbol-spaced MMSE-DFE which can compensate multiple CFOs was developed based on the SMF model. When a wideband receiving filter is employed to accommodate large CFOs, a FS-DFE [18] should be adopted.

Let L_c and L_b be the lengths in symbols of the feedforward and feedback filters, respectively of the FS-DFE, let Δ be the delay at the decision output, and Γ be the length in symbols of the equivalent channel impulse response. Γ is upper bounded by the sum of the length of the impulse response $g_T(t)$ and the maximum integer value for delay that the relays can choose.

We introduce the following vector notation:

$$\mathbf{a}_k = [a_k, \cdots, a_{k-\Gamma-L_c+1}]^T$$
$$\underline{\mathbf{w}}_k = [w_{kF_0+(F_0-1)}, \cdots, w_{kF_0}]$$
$$\mathbf{w}_k = [\underline{\mathbf{w}}_k, \cdots, \underline{\mathbf{w}}_{k-\Gamma-L_c+1}]^T$$
$$\underline{\mathbf{r}}_k = [r_{kF_0+(F_0-1)}, \cdots, r_{kF_0}]$$
$$\mathbf{r}_k = [\underline{\mathbf{r}}_k, \cdots, \underline{\mathbf{r}}_{k-\Gamma-L_c+1}]^T$$
$$\mathbf{q}_{k,i} = [e^{j2\pi\Delta f_1(kF_0-i)T/F_0}, \cdots, e^{j2\pi\Delta f_M(kF_0-i)T/F_0}]$$
$$\mathbf{q}_k = diag(\mathbf{q}_{k,0}, \mathbf{q}_{k,1}, \cdots, \mathbf{q}_{k,F_0-1})$$
$$\mathbf{Q}_k = diag(\mathbf{q}_k, \mathbf{q}_{k-1}, \cdots, \mathbf{q}_{k-L_c+1})$$

where $diag(\mathbf{a}, \cdots, \mathbf{z})$ denotes the block diagonal matrix with the vectors or matrices $\mathbf{a}, \cdots, \mathbf{z}$ on its diagonal.

$$\mathbf{h}_i = [h^{(1)}_{iF_0+(F_0-1)}, \cdots, h^{(M)}_{iF_0+(F_0-1)}, h^{(1)}_{iF_0+(F_0-2)}, \cdots, h^{(M)}_{iF_0+(F_0-2)}, \cdots, h^{(1)}_{iF_0}, \cdots, h^{(M)}_{iF_0}]^T, \quad i = 0, \cdots, \Gamma-1 \tag{2}$$

$$\mathbf{H} = \begin{bmatrix} \mathbf{h}_0 & \mathbf{h}_1 & \mathbf{h}_2 & \cdots & \mathbf{h}_{\Gamma-1} & \mathbf{0}_{MF_0,1} & \mathbf{0}_{MF_0,1} \cdots \mathbf{0}_{MF_0,1} \\ \mathbf{0}_{MF_0,1} & \mathbf{h}_0 & \mathbf{h}_1 & \cdots & \mathbf{h}_{\Gamma-2} & \mathbf{h}_{\Gamma-1} & \mathbf{0}_{MF_0,1} \cdots \mathbf{0}_{MF_0,1} \\ \mathbf{0}_{MF_0,1} & \mathbf{0}_{MF_0,1} & \mathbf{h}_0 & \cdots & \mathbf{h}_{\Gamma-3} & \mathbf{h}_{\Gamma-2} & \mathbf{h}_{\Gamma-1} \cdots \mathbf{0}_{MF_0,1} \\ \vdots & & \ddots & & & & \ddots \quad \vdots \\ \mathbf{0}_{MF_0,1} & \mathbf{0}_{MF_0,1} & \mathbf{0}_{MF_0,1} \cdots & \mathbf{h}_0 & \mathbf{h}_1 & \cdots & \mathbf{h}_{\Gamma-1} \end{bmatrix}$$

where $\mathbf{H}$ is a $L_c MF_0 \times (\Gamma + L_c - 1)$ matrix.

Then the input signal vector to the feed-forward part of FS-DFE can be expressed in matrix form as

$$\mathbf{r}_k = \mathbf{Q}_k \mathbf{H} \mathbf{a}_k + \mathbf{w}_k$$

The output of the equalizer, in symbol rate, is defined as

$$y_k = \mathbf{c}_k^T \mathbf{r}_k + \mathbf{b}_k^T \hat{\mathbf{a}}_{k-\Delta-1}, \tag{3}$$

where $\hat{\mathbf{a}}_{k-\Delta-1} = [\hat{a}_{k-\Delta-1}, \cdots, \hat{a}_{k-\Delta-L_b}]$ contains the already decided symbols to use in the feedback filter, $\mathbf{c}_k$ and $\mathbf{b}_k$ are the coefficient vectors for the feedforward and feedback filter, respectively.

The coefficient vector $\mathbf{c}_k$ and $\mathbf{b}_k$ can be obtained with [19].

$$\mathbf{c}_k^T = \mathbf{E}_\Delta^H \mathbf{C}^H (\mathbf{C}(\mathbf{I} - \mathbf{D}^H \mathbf{D})\mathbf{C}^H + \frac{\sigma_w^2}{\sigma_x^2}\mathbf{I})^{-1}, \text{ where } \mathbf{C} = \mathbf{Q}_k \mathbf{H}$$

$$\mathbf{b}_k^T = \mathbf{c}_k^T \mathbf{C} \mathbf{D}^H,$$

where $\sigma_x^2 = E[\|a_k\|^2]$ and with the following definition

$$\mathbf{D} = [\mathbf{0}_{L_b \times \Delta} \ \mathbf{I}_{L_b \times L_b} \ \mathbf{0}_{L_b \times (\Gamma + L_c - 1 - L_b - \Delta)}]$$

$\mathbf{E}_\Delta^H = [0 \cdots 0 \, 1 \, 0 \cdots 0]$, where the Δth element is 1.

IV. Simulation Results

In this section we analyze the FS-DFE performance assuming $\mathbf{H}$ and $\mathbf{Q}_k$ are estimated perfectly. We compare to the symbol-rate DFE with matched filter front-end design in [15], in which we model the actual distorted response of the RRC filter receiver when a large CFO is present. The FS-DFE performance with practical estimators for $\mathbf{H}$ and $\mathbf{Q}_k$ will be treated in the next section.

We use Monte-Carlo simulation to get the bit error rate (BER) over delay diversity channels for the 2-relay and 3-relay cases. The results are shown in Fig. 4. It is assumed that each path gain is flat Rayleigh fading. For simplicity, the values of delay for the relays are set to be $\tau_1 = 0, \tau_2 = 1, \tau_3 = 2$ where the maximum diversity gain can be obtained. A packet with 1000 random QPSK symbols is generated per trial; 4000 – 10000 trials will be conducted, depending the BER. The transmitting filter time response is truncated to $[-3T, 3T]$.

The BER curves without CFOs are plotted out for reference in Fig. 4. Here we assume $\Delta f_{\max}$ of 0.39 where the CFOs of the relays are uniformly distributed in $[\Delta f_{\max}, -\Delta f_{\max}]$.

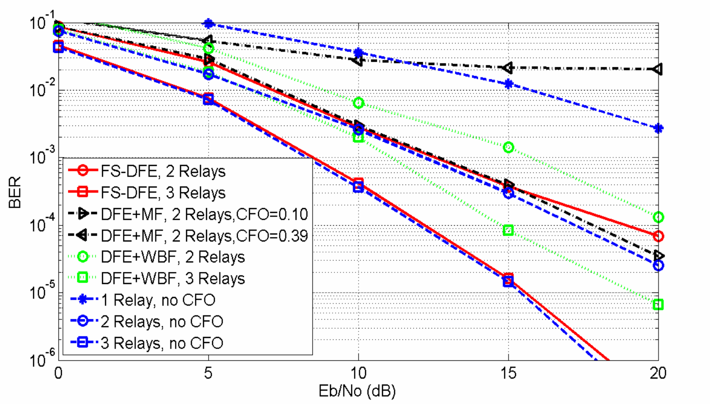

Fig. 4. Comparison between FS-DFE and DFE with random multiple CFOs with perfect channel estimation

The BER performances of the symbol-rate DFE under the matched filter front-end model in [15] for the 2-relay case, denoted as "DFE+MF" in Fig. 4, are shown for $\Delta f_{\max}$ of 0.1 and 0.39. The degradation is small when $\Delta f_{\max}$ is only 0.1, but prominent when $\Delta f_{\max}$ is as large as 0.39. The BERs of FS-DFE under multiple CFOs are very close to those under no CFOs. Symbol-rate DFE also works under our wideband front-end model, but the BERs, denoted as "DFE+WBF" in Fig. 4, are 2-3dB worse than the FS-DFE under multiple CFOs. This is because symbol-rate DFE suffers from noise aliasing when wideband receiving filter $F(\omega)$ is employed.

V. Practical Frequency Offset and Channel Estimation

A. Frame Structure

In the above section, it is shown that the FS-DFE can effectively compensate the effect of multiple CFOs, when these CFOs are exactly known. However, in practice, all the parameters, including the CFOs and the channel gains, should be estimated on the receiver side.

In this section, we propose a frame structure with preambles to accomplish this estimate for burst mode transmission, and the packet error rate (PER) is analyzed.

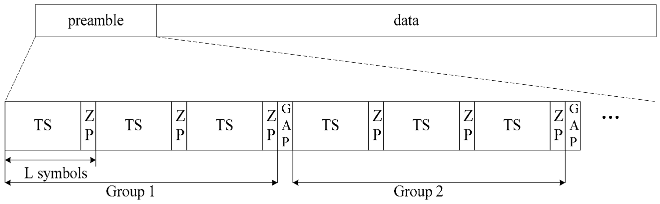

Fig. 5. Frame structure

The frame shown in Fig. 5 consists of the preamble segment and the data segment. The preamble is further divided into groups. Each group is used to estimate the parameters for one relay. Each group consists of several repetitions of a training sequence (TS), which is a BPSK modulated 32 bits M-sequence. Zero padding (ZP) is added between the TSs to eliminate the influence of tails generated by pulse shaping.

The data segment consists of 1024 uncoded symbols for QPSK modulation. Define payload efficiency as the percentage of the data part in the frame. If each group consists of three repeated TSs, then the payload efficiency is about 82% when there are 2 groups, and about 75% when there are 3 groups.

B. Estimation and Tracking Algorithm

For a burst mode transmission, the destination node should proceed with parameter estimation. First, Schimdl's approach [20] is applicable to frame detection. In this paper, we assume perfect frame detection. Then, **t**he frequency offset can be estimated with the repeated TSs [21]; the received preamble can be frequency compensated, and then cross-correlated with the known TS signals to find the position of the peak [21] to get the estimate of timing phase $\hat{t}_0^{(m)}$, and the estimate of channel gain $\hat{\beta}_m$ for the channel between relay R_m and the destination D, then $\hat{h}_k^{(m)}$, the estimate for the channel impulse response, can be obtained using equation (1).

Now all the parameters are estimated and the FS-DFE is applicable for detection. However, because there is always some error in frequency offset estimation, and this will cause large phase error when accumulated over a long time, the phases need to be tracked. A subblock-wise decision-directed adaptive least squares (LS) estimation method was developed to solve this problem.

The data block is segmented into K_S subblocks of length N each, within which the phase rotation is considered to be small and the influence for demodulation is negligible.

The signal model of this LS estimation for the phase errors in the kth subblock is $\mathbf{r}_{Sk} = \sum_{m=1}^{M} \hat{\mathbf{W}}_{Sk}^{(m)} \hat{\mathbf{H}}_{Sk}^{(m)} \hat{\mathbf{a}}_{Sk} g_{Sk}^{(m)}$, where $\mathbf{g}_{Sk} = [g_{Sk}^{(1)}, g_{Sk}^{(2)}, \cdots, g_{Sk}^{(M)}]^T$ is the parameter vector to be estimated, in which the elements are the phase errors relative to different transmitters within the subblock. The subscript S tells this is for the subblock processing, and k represents the kth subblock, the superscript m represents the relay R_m. $\hat{\mathbf{a}}_{Sk} = [\hat{a}_{kN-1}, \cdots, \hat{a}_{(k-1)N}, \hat{a}_{kN-N-1}, \cdots, \hat{a}_{kN-N-\Gamma+1}]^T$ is the detected symbol vector of the kth subblock, and $\mathbf{r}_{Sk} = [r_{kNF_0-1}, \cdots, r_{(k-1)NF_0}]^T$ is the corresponding received signal.

We also define

$$\hat{\mathbf{W}}_{Sk}^{(m)} = diag\,(e^{j2\pi\Delta\hat{f}_m(kNF_0-1)T/F_0}, e^{j2\pi\Delta\hat{f}_m(kNF_0-2)T/F_0}, \cdots, e^{j2\pi\Delta\hat{f}_m(k-1)NF_0T/F_0}),$$

$$\hat{\mathbf{H}}_{Sk}^{(m)} = \hat{\mathbf{H}}_{S(k-1)}^{(m)} \hat{g}_{S(k-1)}^{(m)}, \quad k = 1, 2, \cdots, K_S$$

When $\hat{\mathbf{g}}_{Sk}$ is obtained, the channel impulse response matrix $\hat{\mathbf{H}}_{S(k+1)}^{(m)}$ for the $(k+1)th$ subblock should be updated in this tracking process.

We also define

$$\hat{\mathbf{h}}_i^{(m)} = [\hat{h}_{iF_0+(F_0-1)}^{(m)}, \hat{h}_{iF_0+(F_0-2)}^{(m)}, \cdots, \hat{h}_{iF_0}^{(m)}]^T, \qquad i = 0, \cdots, \Gamma-1 ,$$

$$\hat{\mathbf{H}}_{S0}^{(m)} = \begin{bmatrix} \hat{\mathbf{h}}_0^{(m)} & \hat{\mathbf{h}}_1^{(m)} & \hat{\mathbf{h}}_2^{(m)} & \cdots & \hat{\mathbf{h}}_{(\Gamma-1)}^{(m)} & \mathbf{0}_{F_0,1} & \mathbf{0}_{F_0,1} & \cdots & \mathbf{0}_{F_0,1} \\ \mathbf{0}_{F_0,1} & \hat{\mathbf{h}}_0^{(m)} & \hat{\mathbf{h}}_1^{(m)} & \hat{\mathbf{h}}_2^{(m)} & \cdots & \hat{\mathbf{h}}_{(\Gamma-1)}^{(m)} & \mathbf{0}_{F_0,1} & \cdots & \mathbf{0}_{F_0,1} \\ \mathbf{0}_{F_0,1} & \mathbf{0}_{F_0,1} & \hat{\mathbf{h}}_0^{(m)} & \hat{\mathbf{h}}_1^{(m)} & \hat{\mathbf{h}}_2^{(m)} & \cdots & \hat{\mathbf{h}}_{(\Gamma-1)}^{(m)} & \cdots & \mathbf{0}_{F_0,1} \\ \vdots & & \ddots & & & & \ddots & & \vdots \\ \mathbf{0}_{F_0,1} & \mathbf{0}_{F_0,1} & \mathbf{0}_{F_0,1} & \cdots & \hat{\mathbf{h}}_0^{(m)} & \hat{\mathbf{h}}_1^{(m)} & \hat{\mathbf{h}}_2^{(m)} & \cdots & \hat{\mathbf{h}}_{(\Gamma-1)}^{(m)} \end{bmatrix},$$

and $g_{S0}^{(m)} = 1$, $m = 1, \cdots, M$, for initialization of the tracking.

The expression can be simplified by defining $\mathbf{s}_{Sk}^{(m)} = \hat{\mathbf{W}}_{Sk}^{(m)} \hat{\mathbf{H}}_{Sk}^{(m)} \hat{\mathbf{a}}_{Sk}$ and $\mathbf{S}_{Sk} = [\mathbf{s}_{Sk}^{(1)}, \mathbf{s}_{Sk}^{(2)}, \cdots, \mathbf{s}_{Sk}^{(M)}]$.

Then we get $\mathbf{r}_{Sk} = \mathbf{S}_{Sk}\mathbf{g}_{Sk}$, and the LS estimate for $\mathbf{g}_{Sk}$ is

$$\hat{\mathbf{g}}_{Sk} = (\mathbf{S}_{Sk}^H \mathbf{S}_{Sk})^{-1} \mathbf{S}_{Sk}^H \mathbf{r}_{Sk} \; . \tag{4}$$

The intuition is that the vector $\mathbf{g}_{Sk}$ represents the phase rotation caused by the frequency offset estimation error.

Then before utilizing equation (3) in the equalization process for the kth subblock, instead of using the $\mathbf{h}_i$ defined in equation (2), we use

$$\hat{\mathbf{h}}_{i,Sk} = \hat{\mathbf{h}}_{i,S(k-1)} \circ \mathrm{Rep}_{F_0}\left(\hat{\mathbf{g}}_{S(k-1)}\right), \tag{5}$$

for $i = 0, \cdots, \Gamma-1$ and $k = 1, \cdots, K_S$,

to calculate the channel impulse response matrix $\mathbf{H}$, and the equalizer coefficient vectors $\mathbf{c}_k$ and $\mathbf{b}_k$. Here $\circ$ denotes "element-by-element multiplication" of two vectors, and $\mathrm{Rep}_{F_0}(\cdot)$ is an function to repeat a column vector F_0 times.

$\hat{\mathbf{h}}_{i,Sk}$ is updated per subblock as in (5), and we define $\hat{\mathbf{h}}_{i,S0} = [\hat{h}_{iF_0+(F_0-1)}^{(1)}, \cdots, \hat{h}_{iF_0+(F_0-1)}^{(M)}, \hat{h}_{iF_0+(F_0-2)}^{(1)}, \cdots, \hat{h}_{iF_0+(F_0-2)}^{(M)}, \cdots, \hat{h}_{iF_0}^{(1)}, \cdots, \hat{h}_{iF_0}^{(M)}]^T$ for initialization of the process.

The adaptive tracking mechanism is shown in Fig. 6, where $\hat{\mathbf{h}}_{S1} = [\hat{\mathbf{h}}_{0,S1}, \hat{\mathbf{h}}_{1,S1}, \hat{\mathbf{h}}_{2,S1}, \cdots, \hat{\mathbf{h}}_{\Gamma-1,S1}]$ and $\Delta\hat{\mathbf{f}} = [\Delta\hat{f}_1, \Delta\hat{f}_2, \cdots, \Delta\hat{f}_M]$.

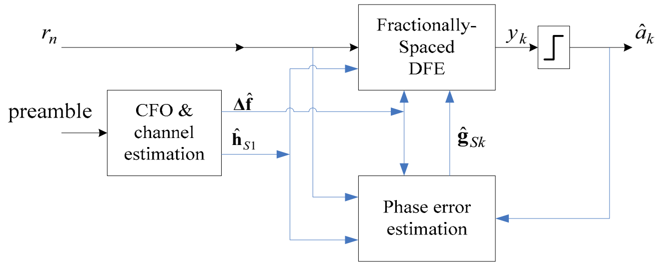

Fig. 6. Adaptive phase tracking

This concept is like a subblock-wise decision-directed phase locked loop, however, several phases are tracked simultaneously.

C. Simulation

Monte-Carlo analysis on packet error rate (PER) is made over delay diversity channels and the results are shown in Fig. 7. The assumptions are the same for the simulation for equalization, however here all the parameters are estimated. An uncoded packet with 1024 random QPSK data symbols is generated per trial, 2000 – 20000 trials are conducted, depending on PER. The burst mode packet is prefixed with a preamble, which is employed for parameter estimation. The 1-relay, 2-relay and 3-relay cases are analyzed, and the PER curves for no CFOs and perfect parameter estimation are also plotted out as a reference.

Two consecutive TSs in the preamble can be employed to estimate frequency offset. When more TSs are available in each group, more accurate frequency offset estimation can be obtained by averaging. The effects of two, three and four TSs in each group in the preamble are also simulated to analyze the effect of the accuracy of estimation.

Because of the estimation error, the PER performance suffers some degradation when compared to those with perfect estimation. When only 2 TSs are used for frequency offset estimation, we can see a 2-3dB gap in the 2-relay case, and about a 7 dB gap in the 3-relay case, when PER is in the region 10E-1 to 10E-2. The PER performance of the 3-relay case is even worse than of the 2-relay case because of estimation error in this region. With more TSs, the frequency offset estimate is more accurate and the PER performance is better; the gap falls into 2.5dB in the 3-relay case, when 4TSs are used.

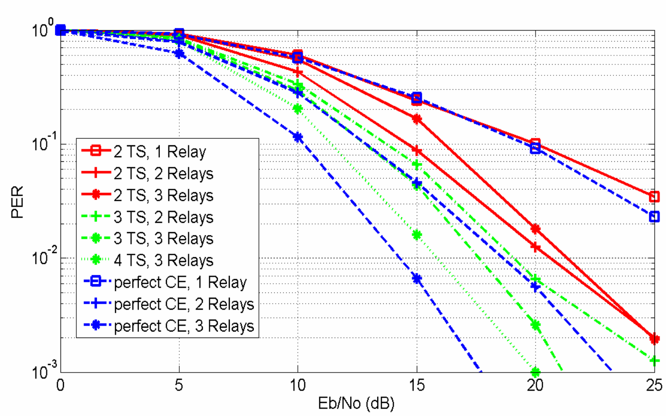

Fig. 7. PER of FS-DFE with channel estimation

VI. Conclusion

A practical equalizer design for cooperative transmission with delay diversity under multiple large CFOs is presented in this paper. Simulation results show that diversity gain is preserved when our proposed approach uses a wider receiver filter followed by a phase-compensated fractionally spaced equalizer. The design can extend to the asynchronous case when the delays are not exactly the multiples of symbol period.

References

[1] J. N. Laneman, D. N. C. Tse, and G. W. Wornell, "Cooperative Diversity in Wireless Networks: Efficient Protocols and Outage Behavior," IEEE Trans. Inform. Theory, vol. 50, no. 12, pp. 3062-3080, Dec. 2004.

[2] A. Sendonaris, E. Erkip, and B. Aazhang, "User cooperation diversity, Part I: System description," IEEE Trans. Commun., vol. 51, pp. 1927–1938, Nov. 2003.

[3] H. Jung, Y. J. Chang, and M. A. Ingram, "Experimental Range Extension of Concurrent Cooperative Transmission in Indoor Environments at 2.4GHz," MILCOM, San Jose, CA, Nov. 2010.

[4] D. Chen, J. N. Laneman, "Noncoherent Demodulation for Cooperative Diversity in Wireless Systems," IEEE Globecom 2004.

[5] T. Himsoon, W. P. Siriwongpairat, W. Su, K. J. Ray Liu, "Differential Modulations for Multinode Cooperative Communications," IEEE Trans. Signal Processing, Vol. 56, No. 7, pp. 2941–2956, July 2008.

[6] J. N. Laneman and G. W. Wornell, "Distributed Space-time-coded protocols for exploiting cooperative diversity in wireless networks," IEEE Trans. Inform. Theory, vol. 49, no. 10, pp. 2415-2525, Oct. 2003.

[7] Y. Jing, H. Jafarkhani, "Distributed Differential Space-Time Coding for Wireless Relay Networks," IEEE Trans. Commun., Vol. 56, No. 7, pp. 1092–1100, July 2008.

[8] F. Oggier, B. Hassibi, "A Coding Scheme for Wireless Networks with Multiple Antenna Nodes and No Channel Information," ICASSP 2007.

[9] B. S. Mergen, A. Scaglione, "Randomized Space-Time Coding for Distributed Cooperative Communication," IEEE Trans. Signal Processing, Volume 55, Issue 10, pp. 5003–5017, Oct. 2007.

[10] J. H. Jang, H. C. Won, G. H. Im, "Cyclic prefixed single carrier transmission with SFBC over mobile wireless channels," IEEE Signal Process. Lett., Vol. 13, No. 5, pp. 261–264, May 2006..

[11] S. Wei, D. L. Goeckel, M. Valenti, "Asynchronous Cooperative Diversity," IEEE Trans. Wireless Commun., Vol. 5, No. 6, pp. 1547–1557, June 2006.

[12] I. Chatzigeorgiou, W. S. Guo, I. J. Wasell, "Comparison of Cooperative Schemes using Joint Channel Coding and High-order Modulation," ISCCSP 2008, Malta, 12-14 March 2008.

[13] T. E. Hunter, A. Nosratinia, "Diversity through coded cooperation," IEEE Trans. Wireless Commun., Vol. 5, No. 2, pp. 283–289, Feb. 2006.

[14] X. Li, F. Ng, T. Han, "Carrier Frequency Offset Mitigation in Asynchronous Cooperative OFDM Transmissions," IEEE Trans. Signal Processing, Vol. 56, No., 2, pp. 675–685, Feb. 2008.

[15] D. Veronesi, D. L. Goeckel, "Multiple Frequency Offset Compensation in Cooperative Wireless Systems," IEEE Globecom 2006.

[16] A. Yilmaz, "Cooperative Diversity in Carrier Frequency Offset," IEEE Commun. Letters, Vol. 11, No. 4, pp. 307–309, April 2007.

[17] ARIB STD-T67 ver. 1.1, http:// www.arib.or.jp

[18] J. G. Proakis, M. Salehi, Digital Communications, 5th Edition, McGraw-Hill, Nov. 2007.

[19] N. Benvenuto and G. Cherubini, Algorithms for Communications System and their Applications, John Wiley & Sons Ltd, Mar. 2003.

[20] T. M. Schmidl, D. C. Cox, "Robust Frequency and Timing Synchronization for OFDM," IEEE Trans. Commun., Vol. 45, No. 12, pp. 1613–1621, Dec. 1997.

[21] S. Hara, R. Prasad, Multicarrier Techniques for 4G Mobile Communications, Artech House, 2003.